

Ultrafast Photophysics of Transition Metal Complexes

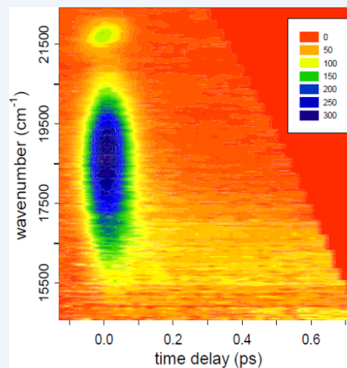
Published as part of the *Accounts of Chemical Research* special issue “Ultrafast Excited-State Processes in Inorganic Systems”.

Majed Chergui*

Ecole Polytechnique Fédérale de Lausanne, Laboratoire de Spectroscopie Ultraprécise, ISIC, Faculté des Sciences de Base, Station 6, CH-1015 Lausanne, Switzerland

CONSPECTUS: The properties of transition metal complexes are interesting not only for their potential applications in solar energy conversion, OLEDs, molecular electronics, biology, photochemistry, etc. but also for their fascinating photophysical properties that call for a rethinking of fundamental concepts. With the advent of ultrafast spectroscopy over 25 years ago and, more particularly, with improvements in the past 10–15 years, a new area of study was opened that has led to insightful observations of the intramolecular relaxation processes such as internal conversion (IC), intersystem crossing (ISC), and intramolecular vibrational redistribution (IVR). Indeed, ultrafast optical spectroscopic tools, such as fluorescence up-conversion, show that in many cases, intramolecular relaxation processes can be extremely fast and even shorter than time scales of vibrations. In addition, more and more examples are appearing showing that ultrafast ISC rates do not scale with the magnitude of the metal spin–orbit coupling constant, that is, that there is no heavy-atom effect on ultrafast time scales. It appears that the structural dynamics of the system and the density of states play a crucial role therein.

While optical spectroscopy delivers an insightful picture of electronic relaxation processes involving valence orbitals, the photophysics of metal complexes involves excitations that may be centered on the metal (called metal-centered or MC) or the ligand (called ligand-centered or LC) or involve a transition from one to the other or vice versa (called MLCT or LMCT). These excitations call for an element-specific probe of the photophysics, which is achieved by X-ray absorption spectroscopy. In this case, transitions from core orbitals to valence orbitals or higher allow probing the electronic structure changes induced by the optical excitation of the valence orbitals, while also delivering information about the geometrical rearrangement of the neighbor atoms around the atom of interest. With the emergence of new instruments such as X-ray free electron lasers (XFELs), it is now possible to perform ultrafast laser pump/X-ray emission probe experiments. In this case, one probes the density of occupied states. These core-level spectroscopies and other emerging ones, such as photoelectron spectroscopy of solutions, are delivering a hitherto unseen degree of detail into the photophysics of metal-based molecular complexes. In this Account, we will give examples of applications of the various methods listed above to address specific photophysical processes.



1. INTRODUCTION

The advent of ultrafast spectroscopy some 25 years ago triggered a real revolution in molecular photochemistry and photophysics due to its ability to probe phenomena on the time scale of molecular vibrations.¹ In the study of condensed phase systems (molecules in solution, proteins, materials), an impressive variety of experimental methodologies has been used and developed, such as pump–probe transient absorption spectroscopy in the visible to the infrared spectral ranges,^{1,2} fluorescence up-conversion,^{3,4} nonlinear optical techniques (photon echo, transient grating),^{5,6} and more recently multidimensional spectroscopies.^{7–13} Many of these have been extended to other spectral ranges, such as the UV for nonlinear^{14,15} and multidimensional spectroscopies,^{16,17} the extreme UV (EUV) for photoelectron spectroscopy (UPS) of liquid samples,^{18,19} or the soft and hard X-ray regions for transient X-ray absorption spectroscopy (XAS)^{20–22} or X-ray emission spectroscopy (XES).^{23–25} In combination with advanced computational methods,^{12,26–29} these tools have

delivered an unsurpassed insight into the ultrafast photo-induced dynamics of molecular systems.

The first event upon absorption of a photon by a large molecule is redistribution of energy among different electronic and vibrational degrees of freedom, which may in some cases lead to unimolecular reactions such as dissociation, predissociation, and isomerization. Otherwise, intramolecular energy redistribution proceeds via different nonradiative processes, such as internal conversion (IC), which is the transition between electronic states of similar spin, intersystem crossing (ISC), which involves states of different spin multiplicities, and intramolecular vibration redistribution (IVR), that is, vibrational energy flow from a given vibrational mode (or modes) to others. All these processes are triggered by modifications of the electronic structure (occupancy of orbitals, oxidation state, valency, etc.) and are accompanied by changes of the geometric

Received: September 30, 2014



ACS Publications

© XXXX American Chemical Society

A

DOI: 10.1021/ar500358q
Acc. Chem. Res. XXXX, XXX, XXX–XXX

structure of the complexes. While energy redistribution processes are well monitored by ultrafast optical methods, the elemental selectivity for both the electronic structure and the geometric structure can only be reached by core-level spectroscopies (XAS, XES, or UPS).

The use of the above ultrafast techniques to study metal complexes has, in the past 10–20 years, led to an increased understanding of their photophysical and photochemical processes. The combination of optical and core-level (X-ray or EUV) spectroscopies has been a game changer in our understanding of the mechanisms underlying the photochemistry and photophysics of metal complexes.³⁰ Here we focus on a few selected examples from our studies of the past ten years to illustrate the power of the above novel methods in delivering new insight into the photophysics of transition metal (TM) complexes.

2. EXPERIMENTAL STRATEGIES

2.1. Transient Absorption (TA) Spectroscopy

The most commonly used technique in ultrafast optical-domain spectroscopy is the pump–probe scheme, which is basically an extension to ultrashort times of the traditional flash photolysis technique.^{31,32} In this scheme, a first (pump) pulse excites the system, triggering a photophysical or photochemical process, and a second (probe) pulse interrogates the evolution of the excited state (or states) by absorption to higher states or by stimulated emission (SE). Both of these signals may overlap each other and also overlap with the transparency of the sample induced by the pump pulse (called ground state bleach, GSB), if the ground state absorption spectrum is in the same spectral range. With the development of nonlinear optics, it has become possible not only to reach very short pulse durations of the order of a few femtoseconds but also and most important to generate ultrashort continua that could be used to probe the dynamics of molecular systems over an extended wavelength range.

2.2. Ultrafast Fluorescence Up-Conversion

Following the ultrafast evolution of excited states by emission is preferable because it removes the problem of overlapping signals that occur in TA spectroscopy and it allows a better visualization of the cascading processes among excited states. In order to reach femtosecond temporal resolution, optical sampling methods such as fluorescence up- or down-conversion are ideal.^{33–35} Indeed, even for very short-lived excited singlet states, there is a nonzero probability of emitting photons, which can be detected if the time window of the detection is adequately narrow. An important improvement to the technique came with the introduction of CCD camera detectors coupled to a monochromator, allowing a polychromatic detection and therefore bringing a significant increase in signal-to-noise and speed of data acquisition.^{36–39} In our setup,⁴⁰ the fluorescence is collected by wide-angle optics and focused onto a nonlinear crystal in which it is mixed with a so-called gate pulse, whose time delay with respect to the pump pulse is controlled by an optical delay stage. The intensity of the signal resulting from the sum- (or difference-) frequency of the gate pulse, and the fluorescence is then recorded as a function of the delay time between pump and gate pulses. Figure 1 illustrates the capability of our setup for the case of $[\text{Ru}(\text{bpy})_3]^{2+}$ in solution, showing how the entire emission spectral profile can be recorded at each time delay.

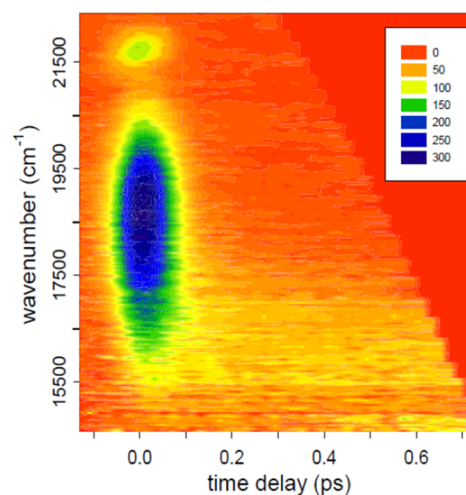


Figure 1. Emission of $[\text{Ru}(\text{bpy})_3]^{2+}$ in water as a function of time upon excitation at 400 nm (25000 cm^{-1}). The signal around $t = 0$ between 16500 and 20000 cm^{-1} is due to the fluorescence of the singlet metal-to-ligand charge transfer ($^1\text{MLCT}$) state, while the yellow stripe centered around 16400 cm^{-1} is due to the $^3\text{MLCT}$ phosphorescence. The spot at 21600 cm^{-1} is the Raman band of the solvent. Reproduced with permission from ref 37. Copyright 2006 Wiley.

2.3. Ultrafast X-ray Absorption Spectroscopy

We have already described this approach in several reviews.^{20,29} Briefly, edges appear in an X-ray absorption spectrum, which correspond to transitions from a core orbital electron (K shell for 1s electrons, L₁ shell for 2s, L₂ for 2p_{1/2}, L₃ for 2p_{3/2} etc.), to the ionization threshold. Just below the edge, one accesses the valence orbitals of the atom, which in the case of coordination chemistry complexes are d orbitals. Thus, XAS probes the density of unoccupied valence states and in a time-resolved experiment, it interrogates the changes therein. For energies above the edge, a photoelectron is produced that scatters off the neighbor atoms, yielding modulations of the spectrum that are due to interferences between different scattering paths (forward, back, and multiple) of the photoelectron wave with the neighbor atoms. These modulations are classified in two regions: the low energy ones (up to $\sim 50 \text{ eV}$ above the edge) are called the X-ray absorption near edge structure (XANES), while at higher energies above the edge they are called the extended X-ray absorption fine structure (EXAFS). These modulations are due to the local structure around the absorbing atom, and any changes in the molecular structure will show up in changes of the XANES and EXAFS.

The implementation of time-resolved XAS was limited to the 50–100 ps temporal widths of X-ray synchrotron pulses.^{41,42} Nevertheless, this time resolution has turned out to be very useful because there are a host of systems whose structural (electronic and geometric) changes were (and still are) unknown upon photoexcitation. To reach the $\sim 100 \text{ fs}$ time resolution, the slicing scheme was implemented at synchrotrons in the soft^{43,44} and hard X-ray⁴⁵ regimes, but the real game changer came with the advent of X-ray free electron lasers,⁴⁶ which deliver ultrashort X-ray pulses with ~ 10 orders of magnitude more photons per pulse than in the slicing scheme. These machines also open the possibility to carry out photon-greedy techniques such as ultrafast X-ray emission spectroscopy (XES), as recently demonstrated on an Fe(II) spin crossover system.²⁵

In this Account, we will mainly focus on our results from a combination of ultrafast and steady-state emission studies and the way they deliver new insight into molecular photophysics.

3. ULTRAFAST IC AND IVR

Over the past few years, we documented a number of TM complexes, where emission from higher lying electronic states was observed.^{47–49} The cases of halogenated rhenium–carbonyl complexes⁴⁷ and more so of the osmium complex Os(dmbp)₃ (dmbp = 4,4'-dimethyl-2,2'-biipyridine) in ethanol⁴⁹ are clear-cut because we could detect intermediate-lived 10–50 ps emissions. In the latter case, it was due to a higher triplet state lying at an energy \sim 2000 cm⁻¹ above the lowest triplet state whose phosphorescence decays in 25 ns, due to a quantum yield of $\leq 5.0 \times 10^{-3}$. The occurrence of such intermediate emissions imply that a weak proportion of population decays radiatively to the ground state, that is, bypassing the lowest electronic excited state.

At the other extreme is the observation of a fluorescence that mirrors the absorption band of the lowest singlet state at the shortest measurable time delays, that is, within the pulse width of the pump laser, and regardless of the excitation energy. This is the case of Figure 1, and it is better depicted in Figure 2,

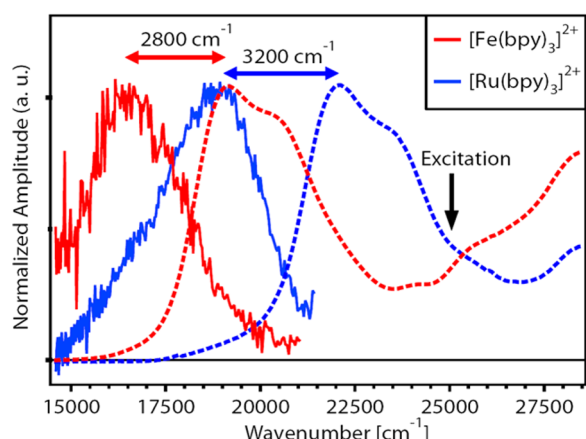


Figure 2. Steady-state absorption spectra showing the ¹MLCT absorption band (dashed traces) and time-zero fluorescence spectra of $[\text{Fe}(\text{bpy})_3]^{2+}$ and $[\text{Ru}(\text{bpy})_3]^{2+}$ in water, excited at 25000 cm^{-1} (black arrow). The horizontal arrows indicate the respective absorption–emission Stokes shift.^{37,50,53} Adapted with permission from ref 50. Copyright 2012 Elsevier.

which shows the absorption bands and the time-zero emission bands of $[\text{Ru}(\text{bpy})_3]^{2+}$ and $[\text{Fe}(\text{bpy})_3]^{2+}$ in solution. Similar observations were made on other Ru complexes⁵⁰ and were found to be independent of the solvent, symmetry of the complex, and initially excited S_n state. The mirror profile of the emission implies that it occurs from a thermalized state, which would seem paradoxical. The lowest singlet fluorescence in Ru- and Fe-polypyridine complexes is found to be very short-lived (<40 fs).⁵⁰ In order to reach the lowest emitting level of the S_1 state, the system has to relax the excess energy via electronic (IC) and vibrational levels (IVR). Taking the lifetime of the ¹MLCT fluorescence as an internal clock, we estimated that the IVR/IC processes occur in <10 fs,⁵⁰ that is, on subvibrational time scales! It should however be stressed that thermalization occurs only with respect to the high frequency Franck–Condon modes that make up the modulations of the

absorption band (Figure 2). These FC modes dump their energy on a subvibrational time scale, in a fashion akin to a critically damped oscillator, into the bath of low frequency, often non-Franck–Condon active modes. When in addition higher S_n states are excited, these very fast relaxation processes must occur in a strongly non-Born–Oppenheimer fashion for the IC to occur, probably involving conical intersections between excited state potential surfaces.⁵¹ These results imply that IC/IVR within singlet states precedes ISC in these systems.

The idea of dumping the energy into low frequency, optically silent modes is difficult to verify in the above examples because the singlet lifetime is too short, but we verified it in the case of organic dyes, such as 2,5-diphenyloxazole (PPO) and *para*-terphenyl (pTP), pumped with a large excess of vibrational energy.^{40,52} It was observed that at zero time delay, the mirror image of the fluorescence with respect to the lowest absorption band is already present but it is structure-less. Thereafter, vibrational cooling of the low frequency modes or solvation dynamics occur on the time scale of several picoseconds, which leads to a structured fluorescence spectrum, identical to the steady-state spectrum.

In conclusion, the observation of a fluorescence that mirror images the absorption of the lowest singlet state at the shortest time delay does not imply ultrafast cooling, except for the high frequency Franck–Condon active modes, because the excess energy is impulsively redistributed into low frequency ones.

4. ULTRAFAST ISC

Figure 1 nicely illustrates the ability of the broad band fluorescence detection at femtosecond resolution to clearly detect the change from fluorescence to phosphorescence for the case of the model complex $[\text{Ru}(\text{bpy})_3]^{2+}$. In the latter,³⁷ as in a whole series of Ru- and Fe-polypyridine complexes we studied,^{50,53} the decay of the ¹MLCT (<40 fs) fluorescence is reflected in the rise of the ³MLCT state. Such ISC times are the shortest ever reported. Further investigations with various transition metal complexes showed that they are uncorrelated to the strength of the spin orbit coupling (SOC) constant, contrary to the expectations based on the so-called “heavy atom effect” known in organic photochemistry.

This is clear from Table 1, which shows the ISC times we measured for various Fe, Ru, Ni, Pt, Pd, Re, and Os complexes.^{37,48–50,53,54} For example, (a) the ISC rate between the lowest singlet and triplet states of a diplatinum complex (Pt₂POP) was found to lie in the 10–30 ps range and to be solvent-dependent!⁴⁸ (b) In complexes such as $[\text{Re}(\text{L})(\text{CO})_3(\text{bpy})]^{n+}$ (for L = Cl, Br, or I, n = 0; for L = etpy (ethylpyridine), n = 1), the ISC times (100–150 fs) are significantly longer than in the Fe or Ru complexes, but remarkably, they decreased in the sequence I, Br, Cl, in what appears as an inverse heavy atom effect.⁴⁷ They also exhibit a linear correlation between the ISC times and the Re–halogen stretch frequency (Figure 3), suggesting that the structural dynamics of the complex mediate the ISC. (c) The comparison between the Fe, Ru, Pt, Re, and Os complexes also underlines the importance of the density of states. For example, Os(dmbp)₃ showed slower ISC times (Figure 4) than Os(bpy)₂(dpp), which has a higher density of states.⁴⁹

The importance of the dynamical aspect of ISC in this temporal regime needs to be stressed. That is, the system explores regions of its configuration space and reaches the points in space where ISC is most favorable due to an energy degeneracy and a favorable coupling of potential surfaces. The

Table 1. Intersystem Crossing Times for the Complexes Investigated by Fluorescence Up-Conversion and Transient Absorption Spectroscopy along with the Spin–Orbit Constant of the Metal Atom

complex	ISC transition	time	spin–orbit constant (eV)	ref
$[\text{Fe}(\text{bpy})_3]^{2+}$	$^1\text{MLCT} \rightarrow ^3\text{MLCT}$	<30 fs	0.05	53
$[\text{Fe}(\text{bpy})_3]^{2+}$	$^3\text{MLCT} \rightarrow ^5\text{T}$	<130 fs		68,69
dithione–dithiolato–Ni	$^1\text{MMLLCT} \rightarrow ^3\text{MMLLCT}$	6 ps	0.095	70
$[\text{Ru}(\text{bpy})_3]^{2+}$	$^1\text{MLCT} \rightarrow ^3\text{MLCT}$	≤ 30 fs	0.1	37
RuN719	$^1\text{MLCT} \rightarrow ^3\text{MLCT}$	≤ 30 fs		50
RuN3	$^1\text{MLCT} \rightarrow ^3\text{MLCT}$	≤ 45 fs		50
dithione–dithiolato–Ni	$^1\text{MMLLCT} \rightarrow ^3\text{MMLLCT}$	6 ps	0.19	70
$[\text{ReX}(\text{CO})_3\text{bpy}]^+$	$^1\text{MLLCT} \rightarrow ^3\text{MLLCT}$		0.335	47
X = Cl		85 fs		
X = Br		130 fs		
X = I		150 fs		
X = etpy		130 fs		
$\text{Os}(\text{dmbp})_3$	$^1\text{MLCT} \rightarrow ^3\text{MLCT}$	100 fs	0.37	49
$\text{Os}(\text{bpy})_2(\text{dpp})$	$^1\text{MLCT} \rightarrow ^3\text{MLCT}$	<50 fs		49
Pt_2POP	$^1\text{A}_{2u} \rightarrow ^3\text{A}_{2u}$	10–30 ps (solvent dependent)	0.583	48
dithione–dithiolato–Pd	$^1\text{MMLLCT} \rightarrow ^3\text{MMLLCT}$	6 ps		70

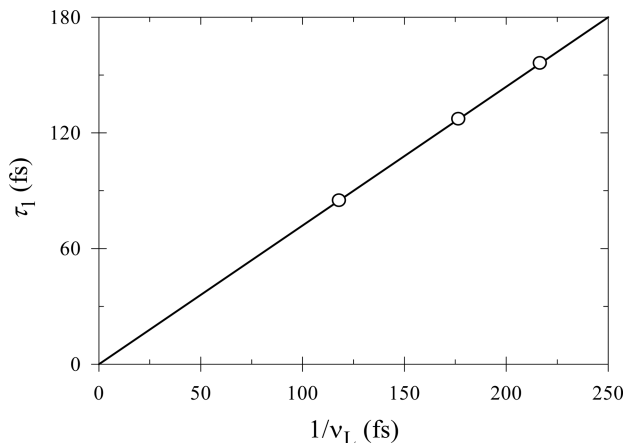


Figure 3. Correlation of the ISC times measured for the $[\text{Re}(\text{L})\text{-}(\text{CO})_3\text{(bpy)}]$ ($\text{L} = \text{Cl}, \text{Br}, \text{I}$, from left to right) complexes⁴⁷ with the vibrational period of the Re–L stretch mode in similar $[\text{Re}(\text{L})\text{-}(\text{CO})_3(\text{iPr-NdCHCHdN-iPr})]$ complexes, as derived from their resonance Raman spectra.⁷¹ Reproduced from ref 47. Copyright 2008 American Chemical Society.

probability of such events is, of course, enhanced if the density of states is high. This is well described in ref 55 and shown in Figure 5. In this respect, the above example with the diplatinum complex illustrates the fact that when the density of states is very low and crossings are unfavorable between states of different multiplicity, the system does not undergo ultrafast ISC, even though it contains two heavy atoms.

Ultrafast ISC also occurs in molecules containing light atoms, and there, the dynamical and energy degeneracy aspects of spin transitions are key parameters, as was beautifully illustrated by Stolow and co-workers in recent ultrafast photoelectron studies of gas phase SO_2 ⁵⁶ and cyclic α, β -enones.⁵⁷ In the first case, they reported ISC from the mixed $^1\text{B}_1 / ^1\text{A}_2$ states to the $^3\text{B}_2$ state on time scales of 750–150 fs, depending on the excitation energy. These were rationalized by Gonzalez and co-workers⁵⁸ using ab initio-based dynamics simulations. It was found that a strong elongation of the SO bonds and a small bending are prerequisites for the ultrafast ISC. In the second case, it was found that upon singlet state excitation of 2-cyclopentenone an

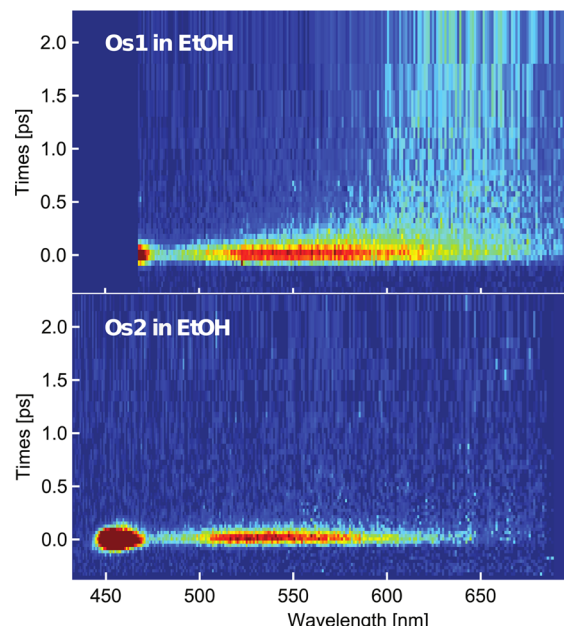


Figure 4. Time–wavelength plots of the emission of $\text{Os}(\text{dmbp})_3$ (Os1) and $\text{Os}(\text{bpy})_2(\text{dpp})$ (Os2) ($\text{dmbp} = 4,4'\text{-dimethyl-2,2'-biipyridine}$, $\text{bpy} = 2,2'\text{-bipyridine}$, $\text{dpp} = 2,3\text{-dipyrindyl pyrazine}$) in ethanol excited at 400 nm. The plots are normalized to the maximum of the fluorescence. The Raman peak at 455 nm is cut on the blue side by the detection window in the top panel. Reproduced from ref 49. Copyright 2013 American Chemical Society.

ISC occurs within 1.2 ps to the lowest triplet manifold, which was explained by a high SOC over an extended region of high singlet–triplet degeneracy explored by the system during its dynamics.

The above considerations should however be mitigated by the fact that in systems with a high spin–orbit coupling (SOC) constant, the classification of states with a pure spin character breaks down. One should rather classify the states as spin–orbit states, as described in ref 28. Of course, the lowest excited states will have a purer spin character because of less mixing, as witnessed by the long phosphorescence lifetimes one measures in luminescent metal complexes. In summary, if a high SOC is

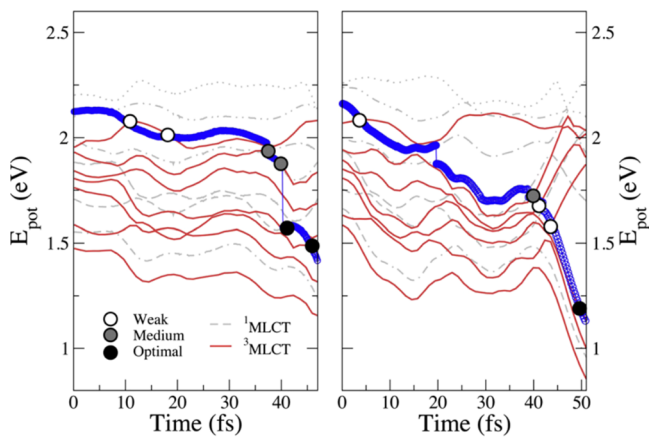


Figure 5. Nonadiabatic molecular dynamics simulations of $[\text{Ru}(\text{bpy})_3]^{2+}$ in solution for the ISC from the $^1\text{MLCT}$ state to the $^3\text{MLCT}$ state. The two panels show the time series of the relevant excited state energies for the two trajectories discussed in the text. Singlet excited states (seven in total) are represented by gray dashed lines and triplet states (seven in total) by red continuous lines.⁵⁵ The driving state is highlighted with blue circles. Analyzed crossings between singlet and triplet states are represented by filled circles with the following color coding: white = weak, gray = medium, and black = optimal SOC strength. See ref 55 for details. Reproduced with permission from ref 55. Copyright 2011 Elsevier.

necessary for high ISC rates, it is not sufficient and parameters such as density of states, crossings of potential surfaces, and structural rearrangements play an important role. In a way, it is similar to electron transfer reactions: a large coupling does not necessarily mean a high rate of electron transfer if the potential surfaces do not have the right crossings. This analogy is actually more relevant than it seems: in $[\text{Fe}(\text{bpy})_3]^{2+}$ the $^3\text{MLCT}-^5\text{T}$ transition occurs in a barrierless region,⁵⁹ while in Pt_2POP , the S and T surfaces are parallel⁴⁸ and are reminiscent of the Marcus inverted region. Finally, $[\text{Re}(\text{L})(\text{CO})_3(\text{bpy})]^{n+}$ complexes would be in the normal region.

5. ELECTRONIC AND MOLECULAR STRUCTURAL CHANGES

In the past few years, we showed how the above processes and their associated electronic and structural changes can be probed with elemental selectivity using time-resolved XAS. We thus successfully identified photoinduced electronic and structural changes in the case of intramolecular electron transfer in Ru-polypyridine,⁶⁰ halogenated Re(I)-carbonyl,⁶¹ and Cu(I)-diimine⁶² complexes, spin crossover³⁰ or photoaquation⁶³ in Fe(II) complexes, photoexcitation of Pt₂ complexes,⁶⁴ and even electron trapping in bare and dye-sensitized TiO₂ nanoparticles.⁶⁵

The halogenated Re(I)-carbonyl complexes are interesting because the ISC, discussed above, is due to a charge transfer excitation, which was predicted to be from the metal–halogen moiety to the bpy ligand. Density functional theory (DFT) had shown that the Re–halogen moiety is strongly mixed:⁴⁷ the $d\pi(\text{Re})$ contribution is between $\sim 53\%$ and $\sim 47\%$ for Cl and Br, respectively, while the corresponding $p\pi(\text{halide})$ contribution is $\sim 18\%$ and $\sim 26\%$. This lead to the classification of the first excited state as MLLCT (metal–ligand-to-ligand charge transfer). The first direct evidence for this character came from picosecond XAS studies that probed the formation of a hole in the Re(5d) and Br(4p) orbitals. Figure 6 shows the Re L₃-edge

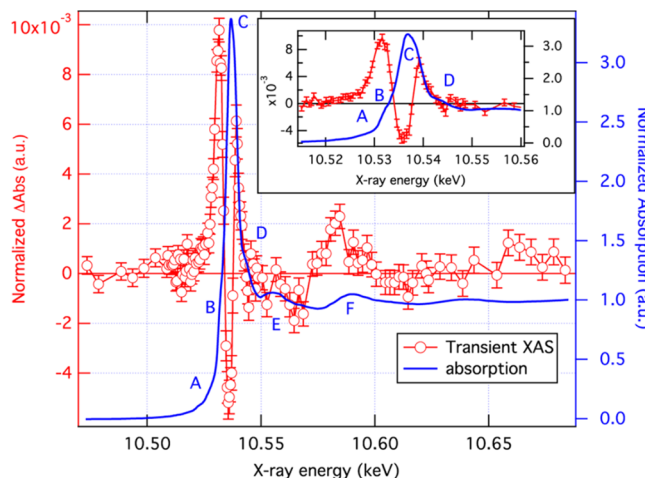


Figure 6. Re L₃-edge transient XAS signal (difference of the excited sample absorption minus the unexcited one) of $[\text{ReBr}(\text{CO})_3(\text{bpy})]$ in solution (red markers) measured 630 ps after excitation at 355 nm. The ground-state XAS (blue line) is shown for comparison with features labeled A–F. Inset: zoom into the near-edge region showing the details of the transient XAS. Reproduced from ref 61. Copyright 2013 American Chemical Society.

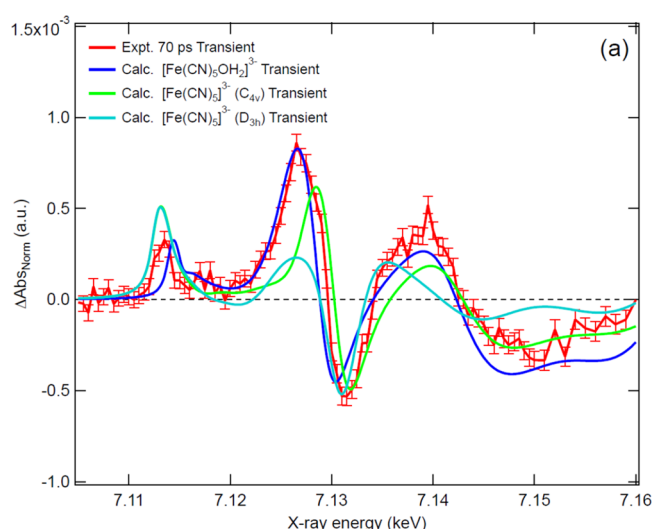


Figure 7. Experimental transient of $[\text{Fe}(\text{CN})_6]^{4-}$ recorded 70 ps after photoexcitation at 355 nm (red) compared with the calculated transient spectra of $[\text{Fe}(\text{CN})_5]^{3-} \text{C}_{4v}$ (green), $[\text{Fe}(\text{CN})_5]^{3-} \text{D}_{3h}$ (cyan), and $[\text{Fe}(\text{CN})_5\text{OH}_2]^{3-}$ (dark blue). Reproduced with permission from ref 63. Copyright 2014 AIP Publishing.

which exhibits a new resonance (B) in the transient just below the edge, because a hole was created in the Re 5d orbital upon MLLCT excitation. The same measurement at the Br K-edge shows formation of a hole in the 4p orbitals.⁶¹ The structural analysis of the XANES and EXAFS regions were in good agreement with the predictions from DFT calculations.^{61,66} This system is ideal for an investigation at ultrashort time scales using XFELs, because the electron transfer, the spin transition, and the structural dynamics are intimately intertwined.

Ferro-hexacyanide is an ideal model system for studying the photoinduced reactivity of a solute with solvent species. Indeed, it has been predicted to undergo photoaquation upon excitation at wavelengths > 310 nm.⁶⁷ However, direct identification of the aquated pentacyano-complex $[\text{Fe}(\text{CN})_5\text{OH}_2]^{3-}$ is

$(\text{CN})_5(\text{OH}_2)]^{3-}$ was so far not possible. We carried out a picosecond XAS study combined with quantum chemical calculations that allowed us to identify this species for the first time.⁶³ Figure 7 shows the transient (difference) spectrum at 70 ps time delay upon 355 nm excitation, along with the calculated transient spectra of different possible photoproducts, demonstrating a best agreement for the aquated pentacyano complex. This system is a very good candidate for XFEL experiments because the route leading to the formation of the latter species is still not known and its elucidation calls for elemental selectivity at high time resolution.

AUTHOR INFORMATION

Corresponding Author

*E-mail: Majed.chergui@epfl.ch.

Funding

This work was supported by the Swiss NSF.

Notes

The authors declare no competing financial interest.

Biography

Majed Chergui is Professor of Physics and Chemistry at the EPFL (Lausanne). He has contributed to the development of several new ultrafast spectroscopic tools, which he uses to study the photoinduced dynamics in metal complexes, in proteins, and in nanoparticles. He is Editor-in-Chief of the new journal *Structural Dynamics*. He recently received the 2015 Earle Plyler Prize of the APS.

REFERENCES

- (1) Zewail, A. H. Femtochemistry: Atomic-scale dynamics of the chemical bond. *J. Phys. Chem. A* **2000**, *104*, 5660–5694.
- (2) McCusker, J. K. Femtosecond absorption spectroscopy of transition metal charge-transfer complexes. *Acc. Chem. Res.* **2003**, *36*, 876–887.
- (3) Gardecki, J.; Horng, M. L.; Papazyan, A.; Maroncelli, M. Ultrafast measurements of the dynamics of solvation in polar and nondipolar solvents. *J. Mol. Liq.* **1995**, *65–66*, 49–57.
- (4) Du, M.; Fleming, G. R. Femtosecond time-resolved fluorescence spectroscopy of bacteriorhodopsin: Direct observation of excited state dynamics in the primary step of the proton pump cycle. *Biophys. Chem.* **1993**, *48*, 101–111.
- (5) Mukamel, S. *Principles of Nonlinear Optical Spectroscopy*; Oxford University Press: New York, 1995.
- (6) Fleming, G. R.; Cho, M. H. Chromophore-solvent dynamics. *Annu. Rev. Phys. Chem.* **1996**, *47*, 109–134.
- (7) Hamm, P.; Zanni, M. T. *Concepts and Methods of 2D Infrared Spectroscopy*; Cambridge University Press: Cambridge, U.K.; New York, 2011.
- (8) Schlau-Cohen, G. S.; Ishizaki, A.; Fleming, G. R. Two-dimensional electronic spectroscopy and photosynthesis: Fundamentals and applications to photosynthetic light-harvesting. *Chem. Phys.* **2011**, *386*, 1–22.
- (9) Ghosh, A.; Hochstrasser, R. M. A peptide's perspective of water dynamics. *Chem. Phys.* **2011**, *390*, 1–13.
- (10) Cannizzo, A. Ultrafast UV spectroscopy: From a local to a global view of dynamical processes in macromolecules. *Phys. Chem. Chem. Phys.* **2012**, *14*, 11205–11223.
- (11) Cho, M. H.; Brixner, T.; Stiopkin, I.; Vaswani, H.; Fleming, G. R. Two dimensional electronic spectroscopy of molecular complexes. *J. Chin. Chem. Soc. (Taipei, Taiwan)* **2006**, *53*, 15–24.
- (12) Mukamel, S.; Tanimura, Y.; Hamm, P. Coherent multidimensional optical spectroscopy. *Acc. Chem. Res.* **2009**, *42*, 1207–1209.
- (13) West, B. A.; Molesky, B. P.; Giokas, P. G.; Moran, A. M. Uncovering molecular relaxation processes with nonlinear spectroscopies in the deep UV. *Chem. Phys.* **2013**, *423*, 92–104.
- (14) Oskouei, A. A.; Braem, O.; Cannizzo, A.; van Mourik, F.; Tortschanoff, A.; Chergui, M. Ultrafast UV photon echo peak shift and fluorescence up conversion studies of non-polar solvation dynamics. *Chem. Phys.* **2008**, *350*, 104–110.
- (15) Ajdarzadeh, A.; Consani, C.; Bram, O.; Tortschanoff, A.; Cannizzo, A.; Chergui, M. Ultraviolet transient absorption, transient grating and photon echo studies of aqueous tryptophan. *Chem. Phys.* **2013**, *422*, 47–52.
- (16) Aubock, G.; Consani, C.; van Mourik, F.; Chergui, M. Ultrabroadband femtosecond two-dimensional ultraviolet transient absorption. *Opt. Lett.* **2012**, *37*, 2337–2339.
- (17) Consani, C.; Aubock, G.; van Mourik, F.; Chergui, M. Ultrafast tryptophan-to-heme electron transfer in myoglobins revealed by UV 2D spectroscopy. *Science* **2013**, *339*, 1586–1589.
- (18) Link, O.; Lugovoy, E.; Siefermann, K.; Liu, Y.; Faubel, M.; Abel, B. Ultrafast electronic spectroscopy for chemical analysis near liquid water interfaces: Concepts and applications. *Appl. Phys. A: Mater. Sci. Process.* **2009**, *96*, 117–135.
- (19) Faubel, M.; Siefermann, K. R.; Liu, Y.; Abel, B. Ultrafast soft X-ray photoelectron spectroscopy at liquid water microjets. *Acc. Chem. Res.* **2012**, *45*, 120–130.
- (20) Chergui, M. Picosecond and femtosecond X-ray absorption spectroscopy of molecular systems. *Acta Crystallogr.* **2010**, *A66*, 229–239.
- (21) Chen, L. X.; Zhang, X. Y.; Lockard, J. V.; Stickrath, A. B.; Attenkofer, K.; Jennings, G.; Liu, D. J. Excited-state molecular structures captured by X-ray transient absorption spectroscopy: A decade and beyond. *Acta Crystallogr.* **2010**, *A66*, 240–251.
- (22) Huse, N.; Cho, H.; Hong, K.; Jamula, L.; de Groot, F. M. F.; Kim, T. K.; McCusker, J. K.; Schoenlein, R. W. Femtosecond Soft X-ray spectroscopy of solvated transition-metal complexes: Deciphering the interplay of electronic and structural dynamics. *J. Phys. Chem. Lett.* **2011**, *2*, 880–884.
- (23) Vanko, G.; Glatzel, P.; Pham, V. T.; Abela, R.; Grolimund, D.; Borca, C. N.; Johnson, S. L.; Milne, C. J.; Bressler, C. Picosecond time-resolved X-ray emission spectroscopy: Ultrafast spin-state determination in an iron complex. *Angew. Chem., Int. Ed.* **2010**, *49*, 5910–5912.
- (24) Bressler, C.; Gawelda, W.; Galler, A.; Nielsen, M. M.; Sundstrom, V.; Doumy, G.; March, A. M.; Southworth, S. H.; Young, L.; Vanko, G. Solvation dynamics monitored by combined X-ray spectroscopies and scattering: photoinduced spin transition in aqueous $[\text{Fe}(\text{bpy})_3]^{2+}$. *Faraday Discuss.* **2014**, *171*, 169–178.
- (25) Zhang, W. K.; Alonso-Mori, R.; Bergmann, U.; Bressler, C.; Chollet, M.; Galler, A.; Gawelda, W.; Hadt, R. G.; Hartsock, R. W.; Kroll, T.; Kjaer, K. S.; Kubicek, K.; Lemke, H. T.; Liang, H. Y. W.; Meyer, D. A.; Nielsen, M. M.; Purser, C.; Robinson, J. S.; Solomon, E. I.; Sun, Z.; Sokaras, D.; van Driel, T. B.; Vanko, G.; Weng, T. C.; Zhu, D. L.; Gaffney, K. J. Tracking excited-state charge and spin dynamics in iron coordination complexes. *Nature* **2014**, *509*, 345–348.
- (26) Ben-Nun, M.; Martinez, T. J. Ab initio quantum molecular dynamics. *Adv. Chem. Phys.* **2002**, *121*, 439–512.
- (27) Tavernelli, I.; Tapavicza, E.; Rothlisberger, U. Non-adiabatic dynamics using time-dependent density functional theory: Assessing the coupling strengths. *J. Mol. Struct. Theochem* **2009**, *914*, 22–29.
- (28) Bakova, R.; Chergui, M.; Daniel, C.; Vlcek, A.; Zalis, S. Relativistic effects in spectroscopy and photophysics of heavy-metal complexes illustrated by spin-orbit calculations of $[\text{Re}(\text{imidazole})(\text{CO})(\text{3})(\text{phen})]^{(+)}$. *Coord. Chem. Rev.* **2011**, *255*, 975–989.
- (29) Milne, C. J.; Penfold, T. J.; Chergui, M. Recent experimental and theoretical developments in time-resolved X-ray spectroscopies. *Coord. Chem. Rev.* **2014**, *277–278*, 44–68.
- (30) Cannizzo, A.; Milne, C. J.; Consani, C.; Gawelda, W.; Bressler, C.; van Mourik, F.; Chergui, M. Light-induced spin crossover in $\text{Fe}(\text{II})$ -based complexes: The full photocycle unraveled by ultrafast

optical and X-ray spectroscopies. *Coord. Chem. Rev.* **2010**, *254*, 2677–2686.

(31) Kirk, A. D.; Hoggard, P. E.; Porter, G. B.; Rockley, M. G.; Windsor, M. W. Picosecond flash-photolysis and spectroscopy - transition-metal coordination-compounds. *Chem. Phys. Lett.* **1976**, *37*, 199–203.

(32) Porter, G. Flash photolysis and spectroscopy a new method for the study of free radical reactions. *Proc. R. Soc. London, Ser. A* **1950**, *200*, 284–300.

(33) Mokhtari, A.; Chesnoy, J.; Laubereau, A. Femtosecond time-resolved and frequency-resolved fluorescence spectroscopy of a dye molecule. *Chem. Phys. Lett.* **1989**, *155*, 593–598.

(34) Arzhantsev, S.; Maroncelli, M. Design and characterization of a femtosecond fluorescence spectrometer based on optical Kerr gating. *Appl. Spectrosc.* **2005**, *59*, 206–220.

(35) Sajadi, M.; Weinberger, M.; Wagenknecht, H. A.; Ernsting, N. P. Polar solvation dynamics in water and methanol: search for molecularity. *Phys. Chem. Chem. Phys.* **2011**, *13*, 17768–17774.

(36) Haacke, S.; Taylor, R. A.; Bar-Joseph, I.; Brasil, M. J. S. P.; Hartig, M.; Deveaud, B. Improving the signal-to-noise ratio of femtosecond luminescence upconversion by multichannel detection. *J. Opt. Soc. Am. B* **1998**, *15*, 1410–1417.

(37) Cannizzo, A.; van Mourik, F.; Gawelda, W.; Zgrablic, G.; Bressler, C.; Chergui, M. Broadband femtosecond fluorescence spectroscopy of $[\text{Ru}(\text{bpy})(3)]^{2+}$. *Angew. Chem., Int. Ed.* **2006**, *45*, 3174–3176.

(38) Zhang, X.-X.; Würth, C.; Zhao, L.; Resch-Genger, U.; Ernsting, N. P.; Sajadi, M. Femtosecond broadband fluorescence upconversion spectroscopy: Improved setup and photometric correction. *Rev. Sci. Instrum.* **2011**, *82*, No. 063108.

(39) Zgrablic, G.; Voitchovsky, K.; Kindermann, M.; Haacke, S.; Chergui, M. Ultrafast excited state dynamics of the protonated Schiff base of all-trans retinal in solvents. *Biophys. J.* **2005**, *88*, 2779–2788.

(40) Cannizzo, A.; Bram, O.; Zgrablic, G.; Tortschanoff, A.; Oskouei, A. A.; van Mourik, F.; Chergui, M. Femtosecond fluorescence upconversion setup with broadband detection in the ultraviolet. *Opt. Lett.* **2007**, *32*, 3555–3557.

(41) Saes, M.; Bressler, C.; van Mourik, F.; Gawelda, W.; Kaiser, M.; Chergui, M.; Bressler, C.; Grolimund, D.; Abela, R.; Glover, T. E.; Heimann, P. A.; Schoenlein, R. W.; Johnson, S. L.; Lindenberg, A. M.; Falcone, R. W. A setup for ultrafast time-resolved x-ray absorption spectroscopy. *Rev. Sci. Instrum.* **2004**, *75*, 24–30.

(42) Lima, F. A.; Milne, C. J.; Amarasinghe, D. C. V.; Rittmann-Frank, M. H.; van der Veen, R. M.; Reinhard, M.; Pham, V. T.; Karlsson, S.; Johnson, S. L.; Grolimund, D.; Borca, C.; Huthwelker, T.; Janousch, M.; van Mourik, F.; Abela, R.; Chergui, M. A high-repetition rate scheme for synchrotron-based picosecond laser pump/x-ray probe experiments on chemical and biological systems in solution. *Rev. Sci. Instrum.* **2011**, *82*, No. 063111.

(43) Schoenlein, R. W.; Chattopadhyay, S.; Chong, H. H. W.; Glover, T. E.; Heimann, P. A.; Shank, C. V.; Zholents, A. A.; Zolotorev, M. S. Generation of femtosecond pulses of synchrotron radiation. *Science* **2000**, *287*, 2237–2240.

(44) Khan, S.; Holldack, K.; Kachel, T.; Mitzner, R.; Quast, T. Femtosecond undulator radiation from sliced electron bunches. *Phys. Rev. Lett.* **2006**, *97*, No. 074801.

(45) Beaud, P.; Johnson, S. L.; Streun, A.; Abela, R.; Abramsohn, D.; Grolimund, D.; Krasniqi, F.; Schmidt, T.; Schlott, V.; Ingold, G. Spatiotemporal stability of a femtosecond hard-X-ray undulator source studied by control of coherent optical phonons. *Phys. Rev. Lett.* **2007**, *99*, No. 174801.

(46) Chergui, M. Emerging photon technologies for chemical dynamics. *Faraday Discuss.* **2014**, *171*, 11–40.

(47) Cannizzo, A.; Blanco-Rodriguez, A. M.; El Nahhas, A.; Sebera, J.; Zalis, S.; Vlcek, A.; Chergui, M. Femtosecond fluorescence and intersystem crossing in rhenium(I) carbonyl-bipyridine complexes. *J. Am. Chem. Soc.* **2008**, *130*, 8967–8974.

(48) van der Veen, R. M.; Cannizzo, A.; van Mourik, F.; Vlcek, A.; Chergui, M. Vibrational relaxation and intersystem crossing of binuclear metal complexes in solution. *J. Am. Chem. Soc.* **2011**, *133*, 305–315.

(49) Bram, O.; Messina, F.; Baranoff, E.; Cannizzo, A.; Nazeeruddin, M. K.; Chergui, M. Ultrafast relaxation dynamics of osmium-polypyridine complexes in solution. *J. Phys. Chem. C* **2013**, *117*, 15958–15966.

(50) Bram, O.; Messina, F.; El-Zohry, A. M.; Cannizzo, A.; Chergui, M. Polychromatic femtosecond fluorescence studies of metal-polypyridine complexes in solution. *Chem. Phys.* **2012**, *393*, 51–57.

(51) Domcke, W.; Yarkony, D.; Köppel, H. *Conical Intersections: Electronic Structure, Dynamics & Spectroscopy*; World Scientific: River Edge, NJ, 2004.

(52) Braem, O.; Penfold, T. J.; Cannizzo, A.; Chergui, M. A femtosecond fluorescence study of vibrational relaxation and cooling dynamics of UV dyes. *Phys. Chem. Chem. Phys.* **2012**, *14*, 3513–3519.

(53) Gawelda, W.; Cannizzo, A.; Pham, V. T.; van Mourik, F.; Bressler, C.; Chergui, M. Ultrafast nonadiabatic dynamics of $[\text{Fe}^{II}(\text{bpy})(3)]^{2+}$ in solution. *J. Am. Chem. Soc.* **2007**, *129*, 8199–8206.

(54) Chergui, M. On the interplay between charge, spin and structural dynamics in transition metal complexes. *Dalton Trans.* **2012**, *41*, 13022–13029.

(55) Tavernelli, I.; Curchod, B. F. E.; Rothlisberger, U. Nonadiabatic molecular dynamics with solvent effects: A LR-TDDFT QM/MM study of ruthenium (II) tris (bipyridine) in water. *Chem. Phys.* **2011**, *391*, 101–109.

(56) Wilkinson, I.; Boguslavskiy, A. E.; Mikosch, J.; Bertrand, J. B.; Worner, H. J.; Villeneuve, D. M.; Spanner, M.; Patchkovskii, S.; Stolow, A. Excited state dynamics in SO_2 . I. Bound state relaxation studied by time-resolved photoelectron-photoion coincidence spectroscopy. *J. Chem. Phys.* **2014**, *140*, No. 204301.

(57) Schalk, O.; Schuurman, M. S.; Wu, G. R.; Lang, P.; Mucke, M.; Feifel, R.; Stolow, A. Internal conversion versus intersystem crossing: What drives the gas phase dynamics of cyclic α,β -enones? *J. Phys. Chem. A* **2014**, *118*, 2279–2287.

(58) Mai, S.; Marquetand, P.; Gonzalez, L. Non-adiabatic and intersystem crossing dynamics in SO_2 . II. The role of triplet states in the bound state dynamics studied by surface-hopping simulations. *J. Chem. Phys.* **2014**, *140*, No. 204302.

(59) de Graaf, C.; Sousa, C. Study of the light-induced spin crossover process of the $[\text{Fe}^{II}(\text{bpy})(3)]^{2+}$ complex. *Chem.—Eur. J.* **2010**, *16*, 4550–4556.

(60) Gawelda, W.; Johnson, M.; de Groot, F. M. F.; Abela, R.; Bressler, C.; Chergui, M. Electronic and molecular structure of photoexcited $[\text{Ru}^{II}(\text{bpy})_3]^{2+}$ probed by picosecond X-ray absorption spectroscopy. *J. Am. Chem. Soc.* **2006**, *128*, 5001–5009.

(61) El Nahhas, A.; van der Veen, R. M.; Penfold, T. J.; Pham, V. T.; Lima, F. A.; Abela, R.; Blanco-Rodriguez, A. M.; Zalis, S.; Vlcek, A.; Tavernelli, I.; Rothlisberger, U.; Milne, C. J.; Chergui, M. X-ray absorption spectroscopy of ground and excited rhenium-carbonyl diimine-complexes: Evidence for a two-center electron transfer. *J. Phys. Chem. A* **2013**, *117*, 361–369.

(62) Penfold, T. J.; Karlsson, S.; Capano, G.; Lima, F. A.; Rittmann, J.; Reinhard, M.; Rittmann-Frank, M. H.; Braem, O.; Baranoff, E.; Abela, R.; Tavernelli, I.; Rothlisberger, U.; Milne, C. J.; Chergui, M. Solvent-induced luminescence quenching: Static and time-resolved X-ray absorption spectroscopy of a copper(I) phenanthroline complex. *J. Phys. Chem. A* **2013**, *117*, 4591–4601.

(63) Reinhard, M.; Penfold, T. J.; Lima, F. A.; Rittmann, J.; Rittmann-Frank, M. H.; Abela, R.; Tavernelli, I.; Rothlisberger, U.; Milne, C. J.; Chergui, M. Photooxidation and photoaquation of iron hexacyanide in aqueous solution: A picosecond X-ray absorption study. *Struct. Dyn.* **2014**, *1*, No. 024901.

(64) van der Veen, R. M.; Kas, J. J.; Milne, C. J.; Pham, V. T.; El Nahhas, A.; Lima, F. A.; Vithanage, D. A.; Rehr, J. J.; Abela, R.; Chergui, M. L-edge XANES analysis of photoexcited metal complexes in solution. *Phys. Chem. Chem. Phys.* **2010**, *12*, 5551–5561.

(65) Rittmann-Frank, M. H.; Milne, C. J.; Rittmann, J.; Reinhard, M.; Penfold, T. J.; Chergui, M. Mapping of the photoinduced electron

traps in TiO₂ by picosecond X-ray absorption spectroscopy. *Angew. Chem., Int. Ed.* **2014**, *53*, 5858–5862.

(66) Zalis, S.; Milne, C. J.; El Nahhas, A.; Blanco-Rodriguez, A. M.; van der Veen, R. M.; Vlcek, A. Re and Br X-ray absorption near-edge structure study of the ground and excited states of [ReBr(CO)₃(bpy)] interpreted by DFT and TD-DFT calculations. *Inorg. Chem.* **2013**, *52*, 5775–5785.

(67) Shirom, M.; Stein, G. Excited state chemistry of ferrocyanide ion in aqueous solution. 2. Photoaquaion. *J. Chem. Phys.* **1971**, *55*, 3379–3382.

(68) Bressler, C.; Milne, C.; Pham, V. T.; El Nahhas, A.; van der Veen, R. M.; Gawelda, W.; Johnson, S.; Beaud, P.; Grolimund, D.; Kaiser, M.; Borca, C. N.; Ingold, G.; Abela, R.; Chergui, M. Femtosecond XANES study of the light-induced spin crossover dynamics in an iron(II) complex. *Science* **2009**, *323*, 489–492.

(69) Consani, C.; Premont-Schwarz, M.; El Nahhas, A.; Bressler, C.; van Mourik, F.; Cannizzo, A.; Chergui, M. Vibrational coherences and relaxation in the high-spin state of aqueous [Fe^{II}(bpy)₃]²⁺. *Angew. Chem., Int. Ed.* **2009**, *48*, 7184–7187.

(70) Frei, F.; Rondi, A.; Espa, D.; Mercuri, M. L.; Pilia, L.; Serpe, A.; Odeh, A.; Van Mourik, F.; Chergui, M.; Feurer, T.; Deplano, P.; Vlcek, A.; Cannizzo, A. Ultrafast electronic and vibrational relaxations in mixed-ligand dithione-dithiolato Ni, Pd, and Pt complexes. *Dalton Trans.* **2014**, *43*, 17666–17676.

(71) Rossenaar, B. D.; Stufkens, D. J.; Vlcek, A. Halide-dependent change of the lowest-excited-state character from MLCT to XLCT for the complexes Re(X)(CO)₃(α -diimine) (X = Cl, Br, I; α -diimine = bpy, iPr-PyCa, iPr-DAB) studied by resonance Raman, time-resolved absorption, and emission spectroscopy. *Inorg. Chem.* **1996**, *35*, 2902–2909.